

Growth and Characterisation of Dilute Antimonide Nitride Materials for Long Wavelength Application

S D Coomber, L Buckle, T Ashley
QinetiQ Ltd., Malvern, Worcestershire, WR14 3PS, UK.

P H Jefferson, D Walker, T D Veal, C F McConville
Dept. of Physics, University of Warwick, Coventry, CV4 7AL, UK

Abstract

The addition of small amounts of nitrogen to III-V semiconductors leads to a large degree of band-gap bowing, giving rise to band-gaps smaller than in the associated binary materials. The addition of a small percentage of nitrogen to GaSb or InSb is predicted to move their response wavelengths into the long or even very long wavelength IR ranges. We report the growth of $Ga_{1-y}In_yN_xSb_{1-x}$ by MBE, using an r.f. plasma nitrogen source. We demonstrate high structural quality, as determined by x-ray diffraction, for $0 \leq y \leq 30\%$ with $x = 1.6 \pm 0.2\%$ material. FTIR absorption measurements show a shift in the cut-off wavelength to longer wavelengths when compared with non indium containing material. Lattice matched growth of $Ga_{0.916}In_{0.084}N_{0.018}Sb_{0.982}$ to GaSb is demonstrated. For InNSb material we demonstrate a reduction in the as grown carrier concentration by annealing, whilst retaining the active nitrogen content. FTIR absorption measurements show the first direct experimental evidence of narrowing of the InSb bandgap due to nitrogen incorporation.

Keywords: Dilute nitride, indium antimonide, InSb, gallium antimonide, GaSb, infrared, MWIR, LWIR

Introduction

The substitution of highly electronegative nitrogen for a few percent of the host anions in a III-V semiconductor leads to a large degree of band-gap bowing, which gives rise to band-gaps smaller than in the associated binary materials¹⁻⁵. The band-gap reduction due to the localised interaction between the host conduction band and the resonant level, can be described by the band anti-crossing (BAC) model⁶.

The electronegativity mismatch between nitrogen and antimony is greater than for any other combination of commonly used group V elements. Consequently the band gap reduction is predicted to move their response wavelengths into the long or even very long wavelength IR ranges, as shown in Figure 1.

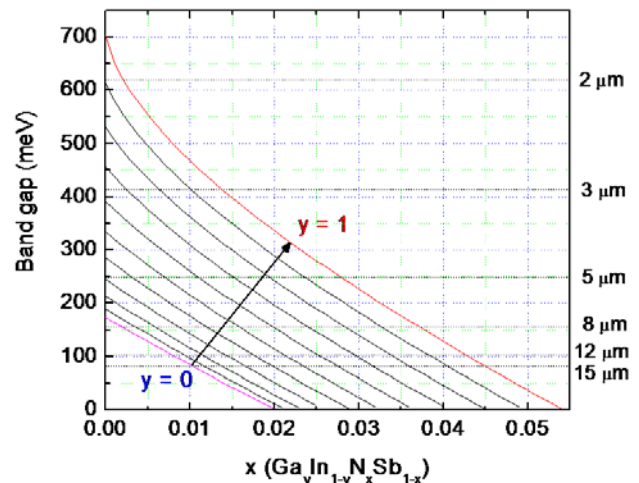


Figure 1 Graph showing bandgap narrowing, and corresponding cut-off wavelength extension, predicted by theory for GaInNSb as the nitrogen content x increases. The two extreme cases shown are for InNSb ($y=0$) and GaNSb ($y=1$).

The dilute III-antimonide nitrides have several potential advantages compared with alternative materials that are sensitive in the mid and long IR wavelength ranges. For example, compared with type-II superlattices, they do not have an InAs component so passivation is easier, and compared with mercury cadmium telluride (MCT), uniformity should be more controllable. Furthermore, there is a theoretical indication that electron effective mass is higher, so diode junction breakdown through tunnelling may be suppressed, which would be particularly important for very long wavelength IR (VLWIR) detection. Finally, as the addition of nitrogen to GaSb decreases the lattice constant, whereas indium increases it, $Ga_{1-y}In_yN_xSb_{1-x}$ offers the prospect of lattice matched growth onto GaSb, InAs or AlSb substrates for multi-band III-V detectors. We have previously^{7,8} demonstrated high structural quality InN_xSb_{1-x} ($x \leq 0.7\%$) and GaN_xSb_{1-x} ($x \leq 1.75\%$) material. However high as grown carrier concentrations, $InNSb$ n type $\sim(2 \pm 1) \times 10^{18} \text{cm}^{-3}$ and $GaN Sb$ p type $\sim(4 \pm 2) \times 10^{18} \text{cm}^{-3}$, necessitated further development for reduction to device compatible levels.

We report the growth of $Ga_{1-y}In_yN_xSb_{1-x}$ by molecular beam epitaxy (MBE), using an r.f. plasma nitrogen source. We examine the influence of indium addition to GaN_xSb_{1-x} with $x = 1.6 \pm 0.2\%$ and investigate the prospect of lattice matching to GaSb substrates. The influence of annealing on the high n type carrier concentration InN_xSb_{1-x} is also investigated, aiming to reduce the carrier concentration to device compatible levels whilst maintaining active nitrogen content. The structural quality of the layers is analysed by X-ray diffraction (XRD) and their optical properties investigated using Fourier transform infra-red (FTIR) absorption spectroscopy. Single field Hall measurements are used to determine the electrical properties of the layers.

Quaternary growth and characterisation

The material has been grown by MBE, using techniques described previously^{9,10}. Standard effusion cells were used for Ga, In and Sb₄. The active nitrogen was supplied by an Oxford Applied Research HD25 plasma source. The samples were of two types: nominally 250nm $Ga_{1-y}In_yN_xSb_{1-x}$ on 250nm $Ga_{1-y}In_ySb$ onto GaSb(001) substrates; or the same $Ga_{1-y}In_yN_xSb_{1-x}$ layer but 2 μm thick grown onto semi insulating GaAs(001) substrates. The samples on GaSb substrates were used for XRD calibration to allow the In content, which increases the lattice constant with respect to the GaSb substrate, to be determined independently of the N content, which conversely decreases the lattice constant. This assumes that the effect of the RF plasma source and subsequent incorporation of N has no effect on the Ga:In ratio. All samples were grown at 360°C with N plasma conditions expected to yield 1.5% N in GaN_xSb_{1-x} . The double crystal X-ray diffraction (DCXRD) was performed, using the symmetric (004) reflection in a Philips diffractometer with Cu K α radiation ($\lambda = 0.15406 \text{ nm}$), and compared with simulated spectra. It should be noted that the majority of these layers were not lattice matched to the GaSb and the intervening layer of GaInSb is beyond critical thickness and will therefore have relaxed.

The layers grown onto GaAs substrates were primarily used for characterisation by Hall effect measurement and FTIR spectroscopy⁸. The use of an insulating substrate that also has a much larger band-gap than the dilute nitride alloys allows the electrical and optical properties to be investigated without being affected by substrate conduction or optical absorption in the wavelength range of interest.

Quaternary $Ga_{1-y}In_yN_xSb_{1-x}$ can be lattice matched to GaSb (and also AlSb as a virtual substrate) by adding the appropriate

amounts of In and N as described in figure 2. Analysis of strain free dilute nitride epilayers would allow accurate determination of the band anti-crossing parameters and it is anticipated that lattice-matching will reduce the threading defect density in the epitaxial films and thus improve the minority carrier lifetimes in the material.

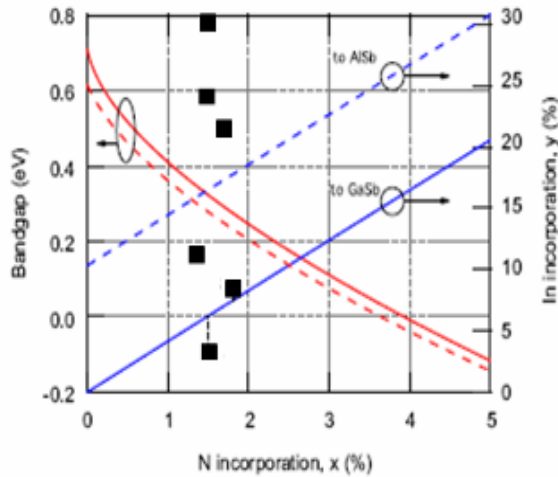


Figure 2 Right hand axis - the indium content as a function of nitrogen incorporation required to maintain a lattice match to GaSb (solid line) and AlSb (dashed line). Left hand axis - the bandgap of GaInNSb alloys lattice matched to GaSb (solid curve) and AlSb (dashed curve) is shown as a function of nitrogen incorporation. The black squares show the In and N concentrations of the samples grown in this study.

An example of the XRD rocking curve for a layer grown on GaSb is shown in figure 3. It shows the three clearly defined layers with the substrate peak in the middle, the GaInSb shifted to the left and the GaInNSb to the right. This sample contained 1.5% N and 3.1% In. It can be seen from figure 3 that 6.2% In would have been required for a lattice matched layer.

An XRD rocking curve of a near lattice matched sample is shown in figure 4. This time the addition of N to the GaInSb has shifted the quaternary XRD peak almost directly on top of the substrate GaSb peak, indicating that close to lattice matching has been achieved.

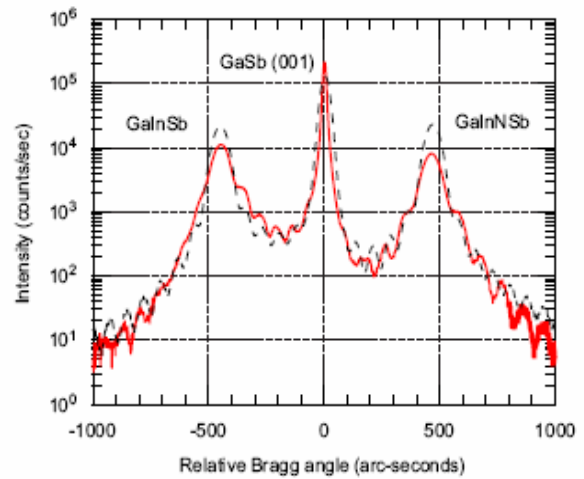


Figure 3. The XRD rocking curve of the 004 diffraction maximum (solid line) together with the dynamical simulation (dashed line) determining Nitrogen and Indium incorporations of 1.5% and 3.1%

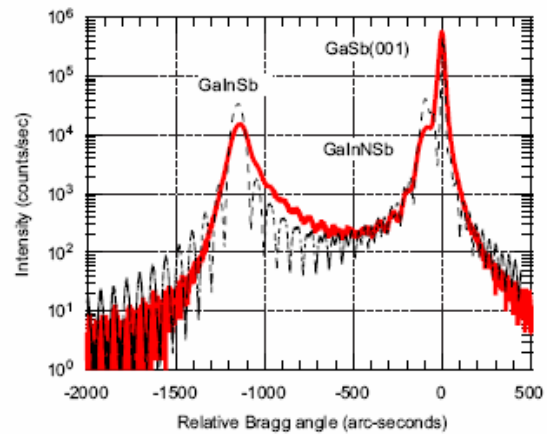


Figure 4. XRD rocking curve of the 004 diffraction maximum (solid line) together with the dynamical simulation (dashed line) determining Nitrogen and Indium incorporations of 1.8% and 7.9% respectively. The GaSb substrate peak can be seen centred at 0 arcsec with the dilute nitride epilayer appearing as a shoulder on this peak indicating a lattice match close to the GaSb substrate.

XRD reciprocal space map analysis was carried out on this sample to quantify any effects of strain on the derived values for the In and N content. It was found that the intermediate GaInSb layer was 12% relaxed while the nitride layer was pseudomorphically grown. The inclusion of strain into the simulation leads to a revision of the In content from 7.9 to $8.4 \pm 0.2\%$ while the N content remained unchanged¹⁰.

The quaternary layers are all heavily p-type at room temperature and 77K. However, there is a slight trend to lower carrier concentrations with increasing In content (see figure 5). This is to be expected due to the high n type character of the InNSb layers.

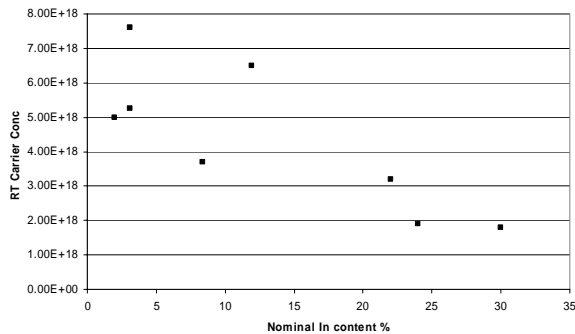


Figure 5. Room temperature Hall data showing carrier concentration as a function of In composition. These layers all contain a nominal $1.6 \pm 0.2\%$ nitrogen.

Figure 6 shows the room temperature infrared transmission spectrum for GaInNSb containing 30% In and 1.5% N. It is compared to spectra for GaSb and GaNSb (1.5% N). Identification of the absorption edge is complicated by the presence of optical interference fringes (for all spectra) and significant absorption below the band gap (for the GaNSb and GaInNSb spectra). This below-gap absorption may be due to impurity or defect states related to the high ($\sim 10^{18}$) p-type background carrier concentration observed in the N containing layers. Analysis of the spectra is continuing in an effort to extract the absorption edge and relate this to the materials band-gap. However a clear trend in the onset of absorption is observed, with a shift to longer wavelength upon introduction of N and a further shift with In incorporation. Qualitatively these absorption shifts agree with theoretical predications for the band-gap narrowing, GaSb = $1.7\mu\text{m}$, GaNSb (1.3%N) = $3.3\mu\text{m}$, GaInNSb (30%In, 1.5%N) = $5\mu\text{m}$.

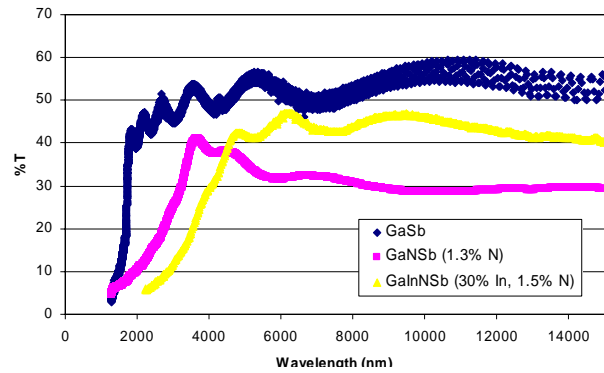


Figure 6 Room temperature FTIR transmission spectra comparing GaSb, GaNSb (1.5%N) and GaInNSb (30%In, 1.5%N)

The $\text{Ga}_{0.916}\text{In}_{0.084}\text{N}_{0.018}\text{Sb}_{0.982}$ near lattice matched sample was re-grown onto a GaSb substrate without the intermediate GaInSb calibration layer. This sample would therefore not have exceeded its critical layer thickness and relaxed like a non lattice matched layer. AFM images of this surface and one from a comparable non-lattice matched GaNSb layer are shown in figure 7. The RMS roughness values are similar but the lattice matched sample does not exhibit the large islands seen on the non-lattice matched layer.

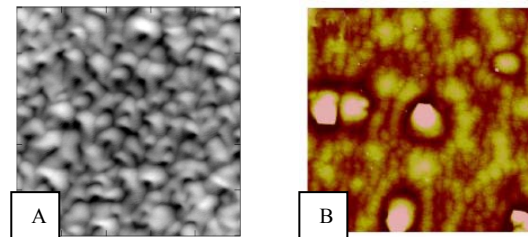


Figure 7. $5 \times 5\mu\text{m}$ AFM images of 250nm thick nitride layers on GaSb substrates. A is the $\text{Ga}_{0.916}\text{In}_{0.084}\text{N}_{0.018}\text{Sb}_{0.982}$ sample lattice matched to GaSb, the height scale is 10nm and the sample had a RMS roughness of 1.8nm. B is a $\text{GaN}_{0.008}\text{Sb}_{0.992}$ sample, the height scale being 5nm and RMS roughness 1.4nm.

InNSb Annealing Investigation

Experiments were carried out for annealing temperatures between 380 and 440°C both *in-situ* and *ex-situ*. To significantly reduce the carrier concentration the annealing temperature had to be in excess of 400°C

but over-annealing resulted in a loss of active nitrogen. Table 1 summarises a subset of results for ex-situ annealing at the most promising temperature of 410°C. It can be seen that it is possible to reduce the carrier concentration to acceptable levels whilst still retaining active nitrogen but there is some variability in the results.

Ex-situ anneal		RT carrier concentration / cm^{-3}	N content / %	N content parent layer / %
Temp / °C	Time / mins			
410	15	1.6×10^{17}	0.36	0.32
410	60	5.3×10^{16}	0.1	0.32
410	60	3.0×10^{17}	0.4	0.55
410	60	2.6×10^{17}	0.1	0.72

Table 1. Ex-situ annealing results for InNSb samples. Unannealed samples have a RT carrier concentration of $\sim 2 \times 10^{18} \text{ cm}^{-3}$ for comparison whilst low temperature grown InSb has a carrier concentration of $\sim 2 \times 10^{16} \text{ cm}^{-3}$.

Figure 8 shows RT FTIR data from an InNSb layer annealed at 410°C and for comparison the spectra for a non-annealed layer, an undoped InSb layer and an InSb layer doped to a similar level. It can be seen that the absorption cut off for the doped InSb shifts to a higher energy compared with the InSb. This is due to the Moss-Burstein shift associated with the high n-type background carrier concentration. The unannealed InNSb is also shifted to higher energy for the same reason. Identification of the absorption edge is complicated by the presence of optical interference fringes (for all spectra) and significant absorption below the band gap (for the InNSb spectra). This below-gap absorption may be due to impurity or defect states related to the high ($\sim 10^{18}$) n-type background carrier concentration. Annealing the sample results in a shift of the absorption cut-off to lower energy (longer wavelength). This confirms the measured reduction in carrier concentration and is direct evidence that the resulting material now has a band-gap narrower than InSb.

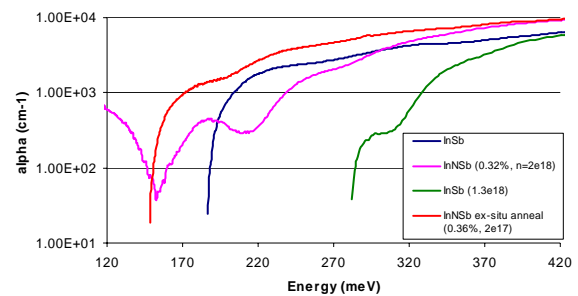


Figure 8. Room temperature FTIR absorption spectra of InNSb and InSb layers

The annealed layers now demonstrate an absorption cut-off energy ($\sim 150 \text{ meV}$) approximately 30 meV lower than that of InSb (180 meV) equivalent to a response wavelength of $\sim 8.5 \mu\text{m}$. This shift in cut-off wavelength is the first direct experimental evidence of narrowing of the InSb band-gap due to N incorporation. Comparison of the experimentally determined cut-off wavelength with the predictions of the band anti-crossing model suggest a N content of $\sim 0.2\%$, which is in qualitative agreement with the XRD measured value of 0.3%.

Conclusions

In summary, initial quaternary growths have demonstrated N and In compositions up to 1.8% and 30% respectively. This material demonstrates a longer cut-off wavelength than for comparable composition GaNSb. Near lattice matching to GaSb has also been demonstrated with a $\text{Ga}_{0.916}\text{In}_{0.084}\text{N}_{0.018}\text{Sb}_{0.982}$ layer. The InNSb as grown carrier concentration has been reduced to $1 \times 10^{17} \text{ cm}^{-3}$ and below by both in-situ and ex-situ annealing. A level suitable for its inclusion as the active layer of a device has therefore been demonstrated. However, more in-situ work is needed to attain a reproducible process because the results are variable as to the nitrogen content retention. FTIR characterisation of the InNSb annealed material has also been carried out and spectra show the removal of the Moss-

Burstein shift seen on the unannealed high carrier concentration layers and a cut-off wavelength clearly shifted to longer wavelengths in agreement with theory predictions.

References

1. M. Weyers, M. Sato and H. Ando, *Jpn. J. Appl. Phys.*, **31**, L853-L855 (1992)
2. H. Naoi, Y. Naoi and S. Sakai, *Solid-State Electron.*, **41**, 319-321 (1997)
3. K. Uesugi, N. Morooka and I. Suemune, *Appl. Phys. Lett.*, **74**, 1254-1256 (1999)
4. W. Shan, W. Walukiewicz, K. M. Yu, J. W. Ager, E.E. Haller, J. F. Geisz, D. J. Friedman, J. M. Olson, S. R. Kurtz and C. Nauka, *Phys. Rev.*, B 62, 4211-4214 (2000)
5. J. Wu, W. Shan and W. Walukiewicz, *Semicond. Sci. Technol.*, **17**, 860-869 (2002)
6. W. Shan, W. Walukiewicz, K. M. Yu, J. W. Ager, E.E. Haller, J. F. Geisz, D. J. Friedman, J. M. Olson, S. R. Kurtz and C. Nauka, *Phys. Rev. Lett.*, **82**, 1221-1224 (1999)
7. P. H. Jefferson, L. Buckle, D. Walker, T. D. Veal, S. Coomber, P. A. Thomas, T. Ashley, C. F. McConville, *Phys. Stat. Sol (RRL)*, 3, 104-106 (2007)
8. L. Buckle, B. R. Bennett, S. Jollands, T. D. Veal, N. R. Wilson, B. N. Murdin, C. F. McConville and T. Ashley, *Proc. 13th Int. Conf on Molecular Beam Epitaxy*, Edinburgh, UK, 2004, *J. Crystal Growth*, 278, 188-192 (2005)
9. T. Ashley, L. Buckle, G. W. Smith, B. N. Murdin, P. H. Jefferson, L. F. J. Piper, T. D. Veal and C. F. McConville, *Proc. SPIE*, **6206**, 62060L (2006)
10. P. H. Jefferson, L. Buckle, B.R. Bennett, T.D. Veal, D. Walker, N.R. Wilson, L.F.J Piper, P.A. Thomas, T.

Ashley, C.F. McConville, *Journal of Crystal Growth*, 304(2) (2007)

Acknowledgements

The work reported in this paper was funded by the Electro-Magnetic Remote Sensing (EMRS) Defence Technology Centre, established by the UK Ministry of Defence and run by a consortium of SELEX Galileo, Thales UK, Roke Manor Research and Filtronic.